Journal of Applied Electrochemistry (2006) 36:1341–1346
DOI 10.1007/s10800-006-9172-5

Photoelectrochemical studies on the *n*-MoS_2–Cysteine interaction

T. MOEHL, M. ABD EL HALIM and H. TRIBUTSCH*
Department of Solar Energy, Hahn-Meitner-Institute, Glienicker Str. 100, D-14109, Berlin, Germany
*(*author for correspondence, e-mail: tributsch@hmi.de)*

Received 17 January 2005; accepted in revised form 27 March 2006

Key words: cysteine, charge transfer, microwave reflection, molybdenum disulfide, semiconductor surface modification

Abstract

The amino acid Cysteine, which plays a significant role as a charge transfer bridge, e.g. in redox proteins like Ferredoxin or Mo-Nitrogenase and in artificial systems like Self Assembled Monolayers (SAM's) on gold, was adsorbed on both, natural and synthetic molybdenum disulfide and the changes were studied with combined photoelectrochemical and microwave conductivity techniques. In contrast to pyrite (FeS_2), where modification with cysteine enhances the electrochemical corrosion, with molybdenum disulfide this is not the case. It was found that cysteine chemically interacts with both dangling bonds of molybdenum on edge sites as well as with d_z^2 orbitals of molybdenum that protrude through the van der Waals surface. The interaction with the edge sites leads to a decrease in dark current and hydrogen evolution activity. In inert electrolyte the interaction with the van der Waals surface leads to a decrease in decomposition-photocurrents due to the action of cysteine as a recombination centre for charge carriers. If, however, a reducing agent such as hydroquinone/quinone or hexacyanoferrate is added, photocurrents increase because the adsorbed cysteine now acts as charge transfer bridge and no longer as a recombination centre. This is supported by a significantly increased microwave conductivity indicating increased charge carrier lifetime.

1. Introduction

Cysteine is an amino acid (Figure 1), which plays a significant role in biological electron transfer related to energy conversion catalysis. It, for example, acts as an electron transfer bridge for the Fe_4S_4 cubane cluster of the Ferredoxin and several other redox proteins [1, 2]. In biosensors cysteine is used as a coupling chain between the inorganic and biological component. It adsorbs with its thiol group on gold and forms Self Assembled Monolayers (SAM's). With its other functional groups it immobilizes redox proteins like Copper–zinc superoxide dismutase (SOD) and acts as a charge transfer chain between the metal and protein [3] or it is capable of promoting redox reactions e.g. of Hydrochinone with Gold [4]. Adsorbed on Titanium dioxide cysteine is able to enhance the reduction of heavy metals along with the destructive oxidation of organic compounds [5, 6] which involves, in both cases, charge transfer via the amino acid. The effect of cysteine on FeS_2 (pyrite) surfaces has been studied in some detail with photoelectrochemical techniques [7]. It was observed that in the presence of cysteine, the anodic dissolution of pyrite is enhanced. The interaction of sulphide oxidizing bacteria (*Acidithiobacillus ferrooxidans*) with pyrite in the presence of cysteine has also been investigated [8], where the amino acid can enhance the availability of FeS_2 as an energy source for these bacteria.

In this study, the interaction of cysteine with molybdenum disulfide crystals should be investigated to achieve deeper understanding, how this amino acid channels charge carriers. If cysteine interacts with the van der Waals surface of this semiconductor a change in interfacial charge transfer could be expected, because the photocurrent flows over these plains [9]. Since photoelectrochemical current voltage curves do not allow a distinction between changes in interfacial electron transfer rate and changes in surface recombination rate, photo-electrochemical studies were combined with light induced microwave conductivity studies. This technique has been described in the literature [10, 11]. Simultaneous measurements of the potential dependent photocurrents and the potential dependent photo microwave conductivity (PMC) reveal additional information on the photoelectrochemical system. The microwave conductivity technique provides a signal proportional to the integral over the number of photogenerated minority carriers $\Delta p(x)$ (here all formulated for a n-type semiconductor) in the semiconductor with the thickness d (1.1). S is a sensitivity factor with

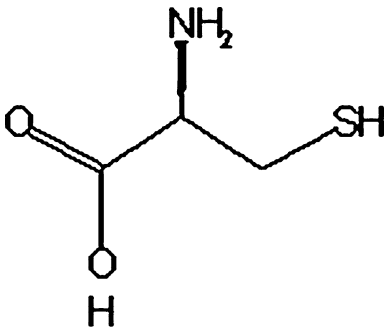

Fig. 1. L-cysteine in its general configuration.

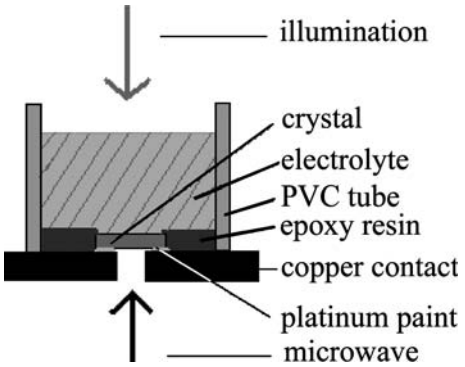

Fig. 2. Photoelectrochemical cell for combined photocurrent-microwave reflection measurements.

the dimension [cm^2]. The measured PMC signal can be related under certain assumptions (in this case low interfacial charge transfer and low surface recombination velocity) to the charge transfer rate k_r and the photo current I_{ph} (1.2):

$$\mathrm{PMC} = \mathrm{S}\int_0^{\mathrm{d}} \Delta p(x)\mathrm{d}x \tag{1.1}$$

$$\frac{k_r}{\Phi(\Delta U)} \infty \frac{I_{ph}}{\mathrm{PMC}} \tag{1.2}$$

$\Phi(\Delta)$ is a function which reflects the minority charge carrier profile in the space charge layer. For a detailed treatment of the theoretical background of microwave reflection measurements at semiconductor-electrolyte interfaces see e.g. [12] and [13]. Qualitatively the PMC signal shows whether the minority carriers accumulate due to a low charge transfer and surface recombination rate constant or whether the minority carriers are depleted under anodic polarization. It is expected that studies on cysteine–metal sulphide interaction will provide deeper knowledge towards charge transfer processes via cysteine. Understanding these processes is important regarding applications for new innovative catalytic centres, interfaces and sensors based on charge transfer via cysteine.

2. Experimental

Natural n-type molybdenum disulfide was obtained via SPI supplies, (http://www.2spi.com/), from a Canadian mine. Synthetic n-type molybdenum disulfide was grown by close space vapour transport. Halogens were used as transport agents and stoichiometric quantities of the elements or the powdery compound itself were used as starting materials [14].

The back contact of the electrochemical cell was made by platinum paint from SPI supplies (sometimes silver epoxy resin was used) and the electrode encapsulated with epoxy resin (Araldit rapid) or silicone (scrintec 901) (Figure 2).

Electrolytes were prepared in with milli-Q water (18 M Ω cm). For measurements free of redox system an electrolyte with 0.5 M K_2SO_4 (Merck, p.a.) was used. For measurements with the redox systems $K_3[Fe(CN)_6]$/$K_4[Fe(CN)_6]$ (both from Merck, p.a.) or Quinone/Hydroquinone (both from Janssen chemika, p.a.) the redox agents were dissolved in 0.5 M K_2SO_4 solution.

To modify the crystals they were dipped in 0.08 M L-cysteine (Fluka, Mikro select > 99.5) solution and left under Nitrogen atmosphere for 14–18 h. The modified electrode was cleaned with milli-Q water.

The combined photocurrent-microwave reflection measurements were performed with 70 Hz chopped illumination through a light guide from a 450-Watt Xenon Lamp (8.6 mW cm^{-2}) or a Schott KL 1500 LCD with a 150 Watt Osram HLX halogen lamp (7.3 mW cm^{-2}). Monochromatic illumination came from a 626 nm LED. The microwave radiation was sent via a wave-guide to the bottom of the photoelectrochemical cell (Figure 2). For a detailed setup see e.g. [10]. The Potential was controlled in a three electrode setup with a SCE (saturated calomel electrode) as reference electrode and a platinum counter electrode. Scanning rates were in the order of 5–20 mV s^{-1}. Photocurrent (via a potentiostat) and microwave reflectance signals (via a rectifying microwave diode) were extracted by Lock-In technique.

A sequence of measurement was carried out as follows:

- First the dark current of the freshly cleaved crystal surface was recorded after several potential prescans.
- Then the photocurrent and microwave reflection were recorded under illumination.
- After the modification (mostly several hours), the measurements of the dark and photocurrent and the microwave reflection were repeated.

3. Results and discussion

3.1. *Dark current measurements:*

Plain cyclic voltammograms of MoS_2 without a modified surface showed that decomposition products such as

oxomolydates (mainly and) can appear at redox potentials around −500 mV vs. SCE. The origin of a commonly appearing broad reduction peak at 0 to −200 mV vs. SCE (Figure 4) is presumably not a sulphur/sulphide reduction peak in contrast to pyrite [7]. No PbS was formed upon addition of $Pb(AC)_2$ and no H_2S found in the applied potential range with differential electrochemical mass spectroscopy (DEMS) measurements. H_2S evolution was only noticed after long (1 min) polarization under high anodic potentials (1.5–2 V vs. SCE). This is a significant difference to the electrochemical behaviour of FeS_2 [7] and to the molybdenum disulfide isostructural compounds tantalum disulfide and titanium disulfide which liberate high quantities of H_2S even under low anodic prepolarisation.

The standard potential $E_0 = -340$ mV vs. NHE at pH = 7 [15] of the redox reaction cysteine/cystine depends strongly on the pH, electrolyte medium and electrode material [16, 17]. No oxidation wave to cystine was observed at cysteine modified MoS_2. When natural MoS_2 was treated with cysteine the anodic corrosion current was reduced as Figures 3, 4 show. This can be attributed to the reduction of surface states and the inhibition of the anodic dissolution of the crystal. When synthetic MoS_2 was treated with cysteine the dark current stays mainly the same because the crystal surface is nearly ideal and only few surface states exist (no figure shown). In molybdenum disulfide surface states originate from unsaturated bonds at the crystal edges (Figure 5). These so called dangling bonds appear as interband energy states located around the Fermi level and are able to trap charge carriers and exchange them with an electrolyte (Figure 6). Cysteine interacts with these bonds especially with those of the molybdenum and saturates them (Figure 5). This leads to a chemical bonding and results in a passivated edge, reduced surface state density and consequently in a lower dark current. A proof for the interaction of these dangling bonds with cysteine can be derived from modification of crystals of different surface quality. If a crystal with a low quantity of imperfections and thus few surface steps is used (which can be determined with an optical microscope) the effect of the modification on the dark current is relatively low, despite the small reduction of the dissolution of the natural sulphide (Figure 4). In contrast to this, crystal surfaces with an optically observed high density of imperfections exhibit higher dark currents. The extreme case when the surface parallel to the *c*-axis, which consists only of sulphur and molybdenum dangling bonds, was exposed to the electrolyte is shown in Figure 3. The decomposition current starting at potentials around 700 mV vs. SCE is

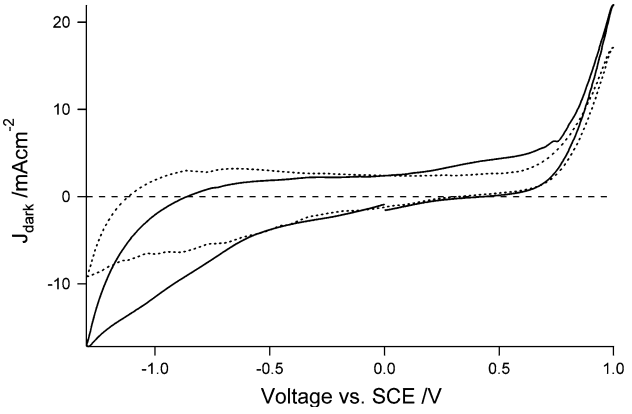

Fig. 3. Cyclic voltammogram of an unmodified (—) and a modified (- -) natural crystal where only the edged planes parallel to the *c*-axis where exposed to 0.5 M K_2SO_4 electrolyte (scan rate 20 mV s^{-1}).

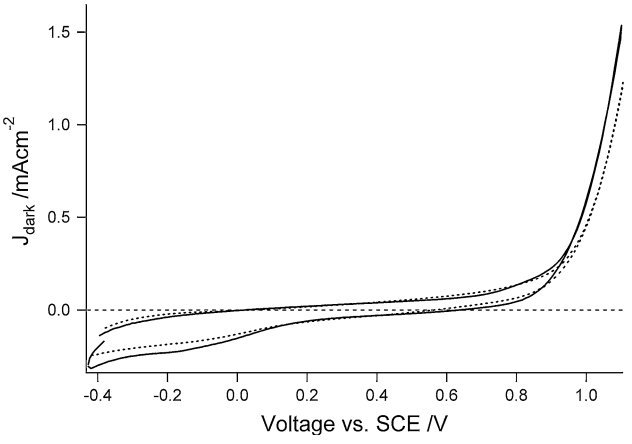

Fig. 4. Cyclic voltammogram of a natural crystal in 0.5 M K_2SO_4 electrolyte before (—) and after (- -) modification (scan rate 50 mV s^{-1}).

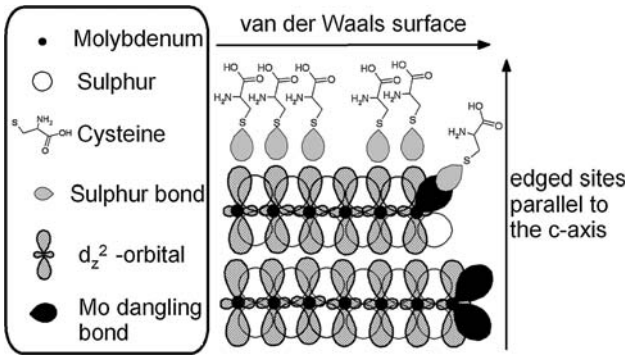

Fig. 5. MoS_2 structure and possible modification places for cysteine.

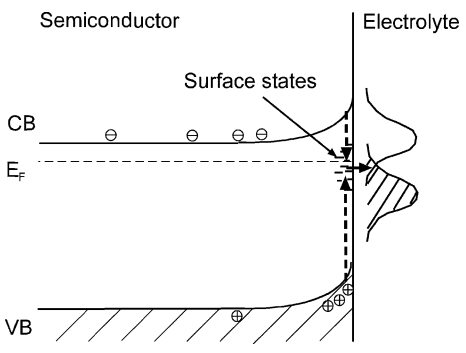

Fig. 6. Band diagram for the charge transfer via the surface states.

reduced. The suppression of the decomposition current itself is based on the blocking of adsorption sites for water and hydroxyl groups. The dissolution of MoS_2 starts with the adsorption of water or hydroxyl groups at Mo(IV) dangling bonds. On the cathodic half cycle hydrogen evolution, starting from −700 mV or lower, is reduced which again finds its origin in the blocking of adsorption sites for water.

3.2. *Photocurrent measurements in inert electrolyte:*

Capacitive surface photovoltage measurements revealed a modification through cysteine by identifying a quenching of the photovoltages lower than the bandgab (inset in Figure 7). This implies an interaction of the thiol with the layered semiconductor and can be ascribed to the reduction of surface state density, which accounts for the appearance of sub-bandgap photovoltages.

In the first series of experiments under illumination only an inert conducting salt was used in the electrolyte. Through this precondition the effect of cysteine on the photocorrosion current could be investigated. In this case all resulting photocurrent can be attributed to the photodissolution of the van der Waals surface with preferences for the edge sites because no redox system is provided for capturing of the charge carriers [18]:

$$MoS_2 + 18h^+ + 12H_2O \rightarrow MoO^{2-}_{4(aq)} + 2SO^{2-}_4 + 24H^+$$

The mechanism of the anodic (photoinduced) dissolution involves several steps and starts with the change of the molybdenum oxidation state from Mo(IV) to Mo(V) at edge sites on the surface. Water or hydroxyl groups (depending on pH) adsorb to the metal and the dissolution starts step after step [19].

After the modification the photocorrosion current was reduced (Figures 8 and 9). Chemisorbed cysteine inhibits the attack and thus the destructive photoreaction. One would be inclined to associate this fact with an increase of charge carriers in the molybdenum disulfide, which would be detectable in the microwave reflection.

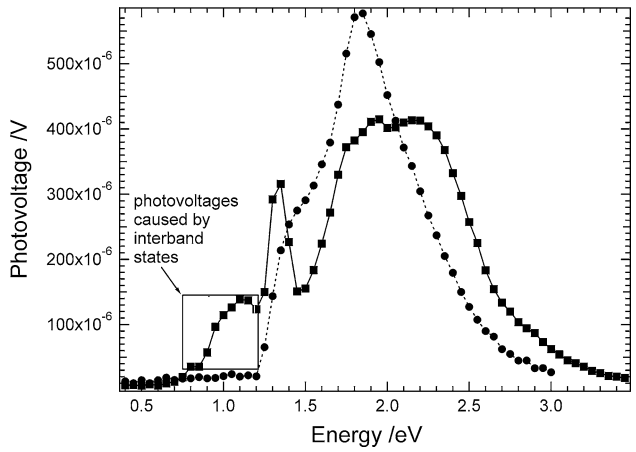

Fig. 7. Photovoltage measurements of a natural MoS_2 crystal (—■— freshly cleaved crystal, –●– cysteine modified crystal).

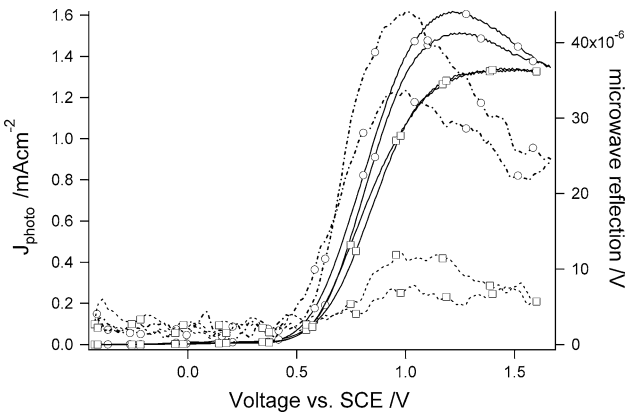

Fig. 8. Decomposition photocurrent (—o—) and microwave reflection (- -o- -) before and after (— □—), (- - □- -) the modification of a natural crystal with cysteine in 0.5 M K_2SO_4 (scan rate 20 mV s^{-1}, lamp: Schott KL).

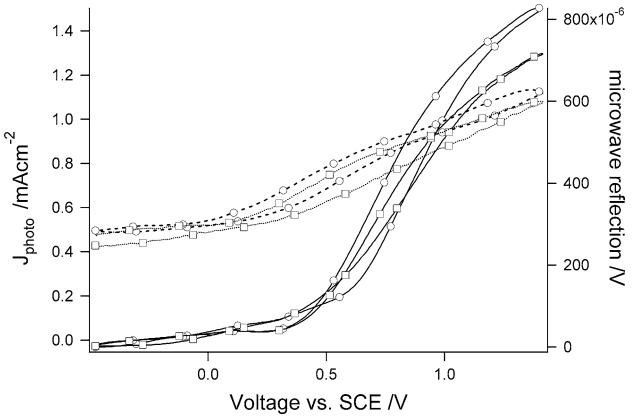

Fig. 9. Decomposition photocurrent (—o—) and microwave reflection (- -o- -) before and after (— □—), (- - □- -) the modification of a synthetic crystal with cysteine in 0.5 M K_2SO_4 with 0.005 M H_2SO_4 (scan rate 20 mV s^{-1}, lamp: Schott KL).

But as both figures show, the microwave reflection was lower, which corresponds to a reduced concentration of charge carriers within the semiconductor. On first sight this result cannot be comprehensively explained only by the modification of the crystal edges. If one takes into account that cysteine acts as a charge transfer chain in nature and biosensors, this results can be described by the capture of holes through the amino acid at the van der Waals surface (Figure 5). Since the photocurrent flows through the van der Waals surface [9] minority carriers must be collected there. This leads to the preliminary conclusion that cysteine interacts with two different bonding sites of the chalcogenide. One weak one (physisorption) at the d_z^2 orbitals protruding through the van der Waals surface [20] where the holes of the n-semiconductors are captured. The other bonding site is the chemisorbed species at the edges of the crystal at the dangling bonds, through which the dark current is channelled. The cysteine interaction with the semiconductors d_z^2 orbitals apparently extracts holes from the valence band and forms an adsorbed intermediate cysteine radical [5] thus lowering the available

holes for the photocorrosion reaction and the amount of free charge carriers in the semiconductor (Figure 10). Simultaneously the recombination increases because the highly reactive positive charge at the semiconductor surface promotes the quenching of excited electronic charge carriers. The charge carriers are subject to a high "surface" recombination in the cysteine molecule, which manifests itself in a reduced microwave reflection. This result is consistent with the reduction of the photovoltage response which identifies higher recombination rates of still hot exited charge carriers towards higher photon energies of modified MoS_2 (Figure 7). The fact that cysteine can interact with two different bonding sites of MoS_2 could also explain the different TDS (thermal desorption spectroscopy) and FT-IR spectra for the modification of molybdenum disulfide with Methylthiol by Mauge et al. [21, 22].

3.3. *Photocurrent measurements with redox electrolyte:*

By adding a redox couple to the electrolyte all resulting photocurrents are not attributed to the dissolution of the disulfide anymore but, in the case of n-type semiconductors to the reduction of photogenerated holes by the reduced form of the redox couple. In the case with a relatively low concentration of redox agent (0.1 M), which still implies low charge transfer and accumulation of charge carriers at the interface (reflected in the microwave signal), cysteine interestingly enhances both the photocurrent and the microwave reflection (Figures 11 and 12). A good example is shown in Figure 12 where a poor charge transfer and a high accumulation of charge carriers were observed at a synthetic crystal. Through the cysteine modification both the photocurrent and the microwave reflection were enhanced. This effect provoked by cysteine can be interpreted as follows: the holes are drawn out from the space charge surface onto the amino acid and are, under these conditions, reduced through electrons offered by the redox couple. The charge transfer between the semiconductor and the reducing agent is assisted by the modification, which results in a higher photocurrent. The increase of the microwave reflection can be interpreted as a loss of recombination centres for photogenerated charges, which leads to a longer lifetime and an accumulation of holes in the space charge. If a reducing agent is offered to the amino acid there are two competing pathways for the holes to react, the recombination or the transfer via cysteine. If the electrolyte offers electrons to the intermediate forming cysteine radical, the charge transfer becomes the governing reaction over the recombination. Thus the function of cysteine as recombination centre for electrons is neutralized and the lifetime of the charge carriers is enhanced.

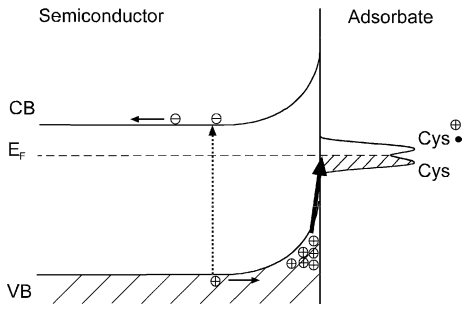

Fig. 10. Band diagram of the cysteine–MoS_2 interaction under illumination.

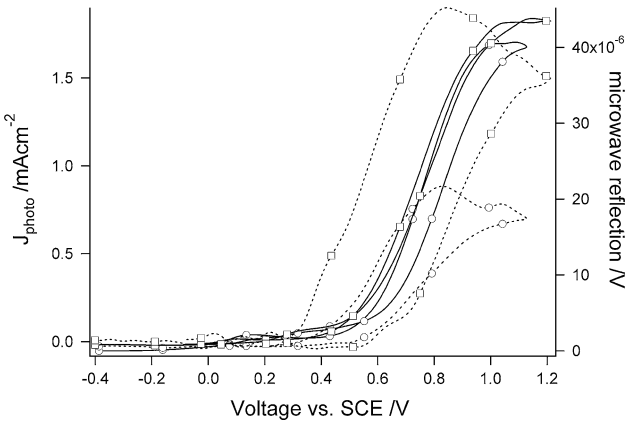

Fig. 11. Photocurrent (—o—) and microwave reflection (- -o- -) before and after (— □—), (- - □- -) the modification of a natural crystal with cysteine in 0.5 M K_2SO_4 with 0.1 M $K_3/K_4[Fe(CN)_6]$ (scan rate 20 mV s^{-1}, xenon lamp).

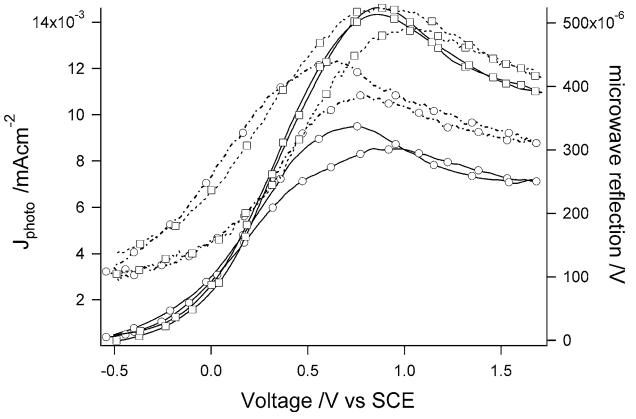

Fig. 12. Photocurrent (—o—) and microwave reflection (- -o- -) before and after (— □—), (- - □- -) the modification of synthetic crystal with cysteine in 0.5 M K_2SO_4 with 0.1 M Hydroquinone (scan rate 20 mV s^{-1}, light intensity of 626 nm LED: 0.9 mW cm^{-2}).

4. Conclusion

In contrast to pyrite, MoS_2 does not dissolve when chemically interacting with cysteine. Cysteine attaches to both the edge sites and the van der Waals surface of MoS_2. The amino acid interacts with the dangling bonds and the through the van der Waals surface protruding d_z^2 orbitals. The interaction decreases the anodic corrosion via modification of the edge sites by occupying the adsorption sites for water. The photocorrosion is

reduced via the modification of the van der Waals surface. This is coupled with the functioning of the physisorbed cysteine as a recombination centre and supported by a low concentration of minority carriers measured via microwave reflection. When a redox couple is added the amino acid acts as pure electron transfer bridge and ceases to function as a surface recombination centre. Therefore the photocurrent is enhanced and due to low recombination via the cysteine the charge carriers can accumulate at the interface. (The determination of the sensitivity factor S which enables a quantitative calculation of a charge transfer constant is complicated and in this series of experiments so far not realised. This should be attempted in a forthcoming paper.)

As shown by these results the MoS_2–cysteine interaction can be used to study and highlight aspects of photoinduced electron transfer via the amino acid.

Acknowledgements

The authors are grateful to Dr. S. Fiechter and Dr. Y. Tomm for fabrication and providing of the synthetic crystals and Dr. T. Dittrich and T. Guminskaya for performing SPV measurements. Special thanks go to S. Seeger, F. Wünsch, P. Bogdanoff and M. Kunst for their time and for fruitful discussions.

References

1. I. Daizadeh, D.M. Medvedev and A.A. Stuchebrukhov, *Mol. Biol. Evol.* **19** (2002) 406.
2. S.J. Lippard and J.M. Berg, *Bioanorganische Chemie* (Spektrum Akademischer Verlag, Heidelberg Berlin Oxford, 1995).
3. Y. Tian, M. Shioda, S. Kasahara, T. Okajima, L. Mao, T. Hisabori and T. Ohsaka, *Biochim Biophys Acta* **1569** (2002) 151.
4. S. Wang and D. Du, *Sens* **2** (2002) 41.
5. T. Rajh, A.E. Ostafin, O.I. Micic, D.M. Tiede and M.C. Thurnauer, *J. Phys. Chem.* **100** (1996) 4538.
6. Rajh T. and Thurnauer M. (2001) Semiconductor assisted metal deposition for nanolithography applications, Pat.-No. 6.271.130, University of Chicago, USA.
7. A.M.A. El-Halim, N. Alonso-Vante and H. Tributsch, *J. Electroanal. Chem.* **399** (1995) 29.
8. J.A. Rojas-Chapana, M. Giersig and H. Tributsch, *Fuel* **75** (1996) 923.
9. Barkschat A., Bildgebende elektrochemische Untersuchungen an Grenzflächen mit metallzentrierten Elektronenübertragungen, Dissertation (Freie University, Berlin, 2004).
10. G. Schlichthorl and H. Tributsch, *Electrochim. Acta* **37** (1992) 919.
11. H. Tributsch, G. Schlichthorl and L. Elstner, *Electrochim. Acta* **38** (1993) 141.
12. Schlichthorl G., Untersuchung der Ladungsträgerkinetik in photoelektrochemische Systemen mit lichtinduzierter Mikrowellenreflektion, Dissertation (Freie Universität, Berlin, 1991).
13. Tributsch H. In White R.E., Conway B.E., Bockris J.O.M. (eds), 'Modern aspects of electrochemistry', vol 33. (Kluwer Academic/Plenum publisher, New York, 1999), pp. 435–522.
14. Bergmann H., Czeska B., Haas I., Mohsin B., and K.-H. Wandner (1992) in Czack G., Katscher H., Kirschstein G., Warkentin E. (eds) Gmelin handbook of inorganic and organometallic chemistry, vol. 7, 8th ed. Springer.
15. Fasman G.D. (1976) in CRC Handbook of Biochemistry and Molecular Biology, Physical Chemical Data, Vol. 1, 3rd ed. (Cleveland, Ohio,), pp. 122–130.
16. T.R. Ralph, M.L. Hitchman, J.P. Millington and F.C. Walsh, *J. Electroanal. Chem.* **375** (1994) 1.
17. T.R. Ralph, M.L. Hitchman, J.P. Millington and F.C. Walsh, *J. Electroanal. Chem.* **275** (1994) 17.
18. F. Decker and B. Scrosati. *in* A. Aruchamy (ed.), Photoelectrochemistry and Photovoltaics of Layered Semiconductors Vol. 14, (Kluwer Academic Publishers, Dordrecht, 1992), pp. 121–154.
19. H. Gerischer and W. Kautek, *J. Electroanal. Chem.* **137** (1982) 239.
20. D. Haneman and H. Tributsch, *Chem. Phys. Lett.* **216** (1993) 81.
21. A.A. Tsyganenko, F. Can, A. Travert and F. Mauge, *Appl. Catal. A* **268** (2004) 189.
22. F. Mauge, J. Lamotte, N.S. Nesterenko, O. Manoilova and A.A. Tsyganenko, *Catal. Today* **70** (2001) 271.